

E. NAGY*[‡], F. KRISTALY**, A. GYENES***, Z. GACSI***

INVESTIGATION OF INTERMETALLIC COMPOUNDS IN Sn-Cu-Ni LEAD-FREE SOLDERS

BADANIE ZWIĄZKÓW MIĘDZYMETALICZNYCH W BEZOŁOWIOWYCH STOPACH LUTOWNICZYCH Sn-Cu-Ni

Interfacial intermetallic compounds (IMC) play an important role in Sn-Cu lead-free soldering. The size and morphology of the intermetallic compounds formed between the lead-free solder and the Cu substrate have a significant effect on the mechanical strength of the solder joint.

In the soldering process of Sn-Cu alloys, Cu_6Sn_5 intermetallic compounds are formed. The complex structural behaviour of Cu_6Sn_5 IMC is temperature- and composition- dependent and it is long since subject to scientific research. The Cu_6Sn_5 phase basically exists in two crystal structures: hexagonal η - Cu_6Sn_5 (at temperatures above 186°C) and monoclinic η' - Cu_6Sn_5 (at lower temperatures). In the presence of Ni in the solder, the η - η' transformation does not occur, therefore, the η - Cu_6Sn_5 phase remains stable.

In this study the role of Ni in the $(\text{Cu},\text{Ni})_6\text{Sn}_5$ intermetallic compound in Sn-Cu lead-free solders was examined. Sn-Cu alloys with different Cu content (0.5 to 1 mass%) were modified through Ni addition. The morphology of the intermetallic compounds of the modified Sn-Cu alloys was investigated by optical microscopy (OM) and scanning electron microscopy (SEM), the IMC phases were examined with X-ray diffraction method (XRD).

Keywords: intermetallics, lead-free solder, X-ray diffraction

1. Introduction

Until recently, lead-containing alloys were considered to be the most suitable soldering materials widely applied in the automotive industry and in several other sectors. However, with the implementation of EU environmental directives (particularly that of RoHS 2011/65/EU), the use of such alloys has become prohibited for negative effects on health. One of the potential alternatives of traditionally used Sn-Sb soldering materials are Sn-Cu based alloys. The most commonly used soldering materials of this alloy family contain 0.5 to 0.9 wt % copper. At a content level of 0.7 wt % copper, an eutectic reaction is known to occur (at 227°C) in the equilibrium binary Sn-Cu system [1, 2]. There is a number of different data on the eutectic composition published by different authors. Moura et al. [3] define the eutectic composition in 0.7 wt. % Cu, while Nogita and others report it to be 0.89 wt. % Cu [4, 5, 6]. In the Sn-rich corner of the alloy phase diagram, the η' - Cu_6Sn_5 phase of monoclinic structure [7] is formed, representing one of the eutectic phases, the other being the β -Sn solid solution. However, at 186°C the η - Cu_6Sn_5 phase undergoes allotropic transformation and evolves into monoclinic η' - Cu_6Sn_5 [8]. This structural transformation from hexagonal structure into monoclinic is accompanied by volume increase (2.15 vol. %). It should be noted that the literature mentions at least four

variants of the Cu_6Sn_5 phase; a new variant has been recently identified [9]. The twofold role of this intermetallic include: the formation of the phase as an interfacial layer between the soldering material and the surface being soldered; and the appearance of the phase in the base material. Certain primary intermetallics, however, are undesirable both in the soldering and the base material. Such is the occurrence of coarse primary $(\text{Cu},\text{Ni})_6\text{Sn}_5$ intermetallic compounds in the microstructure, which may significantly deteriorate the mechanical properties and shorten the lifetime of the solder joint. The formation of these IMCs can be avoided by changing the composition of the alloy.

The η - η' allotropic transformation can be prevented by adding nickel to the Sn-Cu system. Nickel is insoluble in tin; nonetheless, it forms various compounds with copper. Even a small addition of nickel (0.06 m/m %) to the Sn-Cu soldering alloy is able to stabilize the hexagonal η - Cu_6Sn_5 phase. Copper and nickel are mutually substitutable in the compounds formed. The alloying (Ni) atoms occupy suitable positions in the copper lattice to stand for the basic atoms. In the case of the Sn-Cu-Ni system, we talk about $(\text{Cu},\text{Ni})_6\text{Sn}_5$ intermetallic phases. Publications up to date give the following stoichiometry of $(\text{Cu},\text{Ni})_6\text{Sn}_5$ compounds: Gourlay [10] $\text{Cu}_5\text{Ni}_1\text{Sn}_5$, $\text{Cu}_4\text{Ni}_2\text{Sn}_5$, Snugovsky [11] $\text{Cu}_{33}\text{Ni}_{23}\text{Sn}_{44}$,

* MTA-ME MATERIALS SCIENCE RESEARCH GROUP, UNIVERSITY OF MISKOLC, H-3515 MISKOLC-EGYETEMVAROS, HUNGARY

** INSTITUTE OF MINERALOGY AND GEOLOGY, UNIVERSITY OF MISKOLC, H-3515 MISKOLC-EGYETEMVAROS, HUNGARY

*** INSTITUTE OF PHYSICAL METALLURGY, METAL FORMING AND NANOTECHNOLOGY, UNIVERSITY OF MISKOLC, H-3515 MISKOLC-EGYETEMVAROS, HUNGARY

[‡] Corresponding author: femzsofi@uni-miskolc.hu

Vourinen [12] $\text{Cu}_{27}\text{Ni}_{29}\text{Sn}_{44}$. According to literature data, the quantity of dissolved nickel varies in the range of 0-29 at. % for different $(\text{Cu},\text{Ni})_6\text{Sn}_5$ compounds. While studying the Sn-0.7Cu-0.06Ni system, Nogita et al. measured ~9% Ni content in the $(\text{Cu},\text{Ni})_6\text{Sn}_5$ phase [13] and about 5% Ni in the Sn-0.7Cu-0.06Ni system. The $\text{Cu}_4\text{Ni}_2\text{Sn}_5$ phase is the most stable among ternary $\text{Cu}_{6-x}\text{Ni}_x\text{Sn}_5$ phases [6]. Based on IMCs measurements, the $\text{Cu}_{6-x}\text{Ni}_x\text{Sn}_5$ phase has a capacity to dissolve 4.6-17.2% of nickel [14]. According to Gourlay et al., 0 to 25% of dissolved nickel is found in $\text{Cu}_{6-x}\text{Ni}_x\text{Sn}_5$ [10]. Vourinen et al., estimates the Cu/Ni ratio in the intermetallic to be almost the same or slightly higher than in the basic alloy [12]. As for the incorporation of nickel in the lattice, Yu et al. mentions the atomic positions Cu2 or 8f Wyckoff as relevant [15]. Studying the monoclinic Cu_6Sn_5 phase, Gao et al. also identifies the 8f2 position for the Ni atom [16].

In the following investigations, the $(\text{Cu},\text{Ni})_6\text{Sn}_5$ phase was obtained by adding nickel to the Sn-0.7Cu alloy. The goal of this research was to describe the substitution position of dissolved nickel atom in the lattice structure of the copper-based compound. The space required by the substituting nickel atom (after dissolution) is less than that required by the copper atom; therefore, the size of the unit cell decreases, which is studied through the decrease of the lattice parameter.

2. Experimental

Industrial solder ingots of Sn-0.7Cu were used in the experiments to study commercial purity materials. The solder alloy was melted at 400°C in an electric resistance furnace. Different amounts of Ni in the form of SnNi10 master alloy were added to the solder melt. Subsequent to nickel addition and stirring, an incubation time of 30 min was allowed to achieve the complete dissolution of nickel. The alloys were poured into a pre-heated (to 200°C) steel mould of tensile test rods with a diameter of 11 mm. Three samples were casted from each alloy. The chemical compositions of the test samples were analysed by inductively coupled plasma optical emission (ICP-OES) spectrometer and are listed in Table 1.

TABLE 1
Chemical composition of Sn-0.7Cu samples determined by ICP-OES [wt.%]

Sample	Cu	Ni	Ag
Sn-0.7Cu	0.742	0.0005	0.0148
Sn-0.7Cu-0.02Ni	0.737	0.0192	0.0145
Sn-0.7Cu-0.05Ni	0.748	0.0383	0.0178
Sn-0.7Cu-0.1Ni	0.752	0.0820	0.0145
Sn-0.7Cu-0.2Ni	0.743	0.1779	0.0143

The microstructure was observed using a Zeiss AxioVision Imager m1M optical microscope and a Hitachi S4800 scanning electron microscope (SEM). The phase compositions of the samples were measured with a Bruker energy dispersive X-ray spectrometer (EDX) in Laboratory of Physical Metallurgy, Metal Forming and Nanotechnology at University of Miskolc. The XRD measurements were carried out at the Insti-

tute of Mineralogy and Geology of the University of Miskolc, on a Bruker D8 Advance diffractometer equipped with Göbel mirror and position-sensitive detector, with Cu-K α radiation. Bruker DiffracPlus EVA software was used for the evaluation of diffractograms and TOPAS4 for quantitative and structural data obtained by Rietveld refinement.

3. Results and discussion

3.1. Microstructure of Sn-Cu alloys

The microstructure of Sn-0.7 Cu nickel-free alloys contains the dendrites of a β -Sn solid solution and of eutectic β -Sn + Cu_6Sn_5 (Fig. 1.). In Sn-0.7Cu alloys, a very fine, fully eutectic structure is reached already at a Ni content of 1000 ppm. 2000 ppm nickel implies the appearance of primary $(\text{Cu},\text{Ni})_6\text{Sn}_5$ intermetallic phases in the microstructure, which is also supported by the results of EDS measurements. These microstructural differences are well visible in the SEM images presented in Fig. 2.

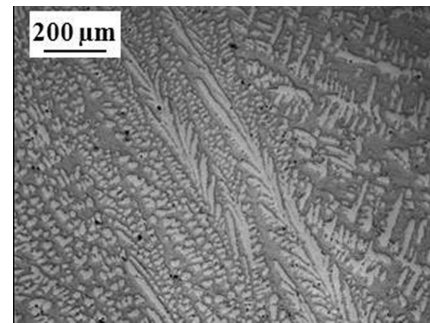


Fig. 1. Microstructure of Sn-0.7Cu sample

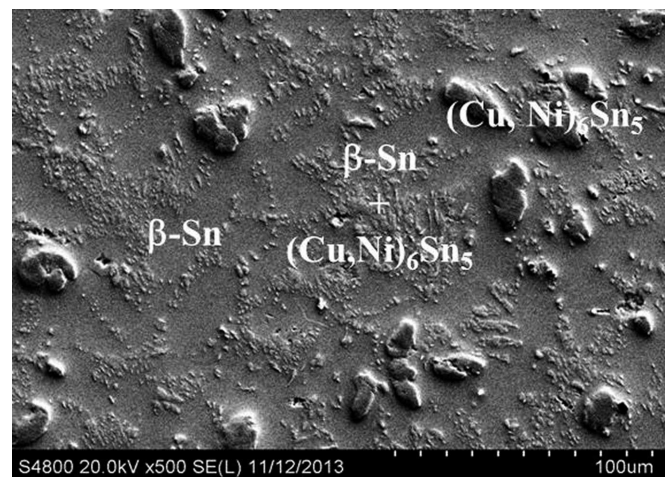


Fig. 2. SEM image of SnCu0.7Ni0.2 alloy with phases depicted

3.2. Simulation of the atomic position of substituting Ni in the η - Cu_6Sn_5 phase

The η - Cu_6Sn_5 phase has hexagonal $P6_3/mmc$ structure (space group No149.). In the Ni_2In -type structure, Cu atoms occupy the Wyckoff positions 2a and 2d (2 atoms per unit cell), while Sn atoms take up the position 2c (2 atoms per

unit cell) (Fig. 3.). The position 2d is partially occupied (0.4 atoms). The lattice parameters are as follows: $a = 4.20062 \text{ \AA}$, $c = 0.50974 \text{ \AA}$ [17]. The incorporation of nickel atoms in one of the four possible Cu sites has been studied primarily by simulation.

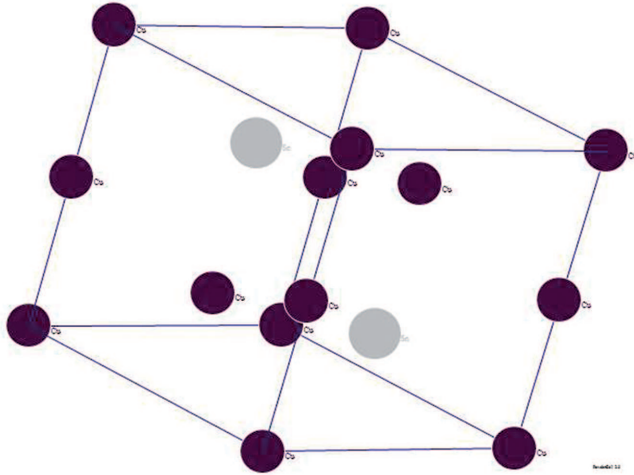


Fig. 3. Unit cell of the Cu_6Sn_5 phase (dark ball-Cu atom, grey ball-Sn atom)

PowderCell 2.4 software was used for the simulation of the atomic positions of nickel atoms incorporation. During the simulation, a diffraction model with no geometry specification was chosen. The simulation of the Bragg-Brentano geometry at large diffraction angles would lead to a decrease in intensity, which would make the interpretation of the simulated full-view diffractogram difficult. First, the Cu_6Sn_5 phase was simulated by the software. The Cu atoms were placed in the fully occupied positions (0,0,0) and (0,0,1/2) and in the partially occupied positions (1/3,2/3,3/4) and (2/3,1/3,1/4). The Sn atoms were placed in the fully occupied positions (1/3,2/3,1/4) and (2/3,1/3,3/4). The possible incorporation of one, two and more atoms in the lattice was studied. The simulation started from the first fully occupied Cu site, then the second fully occupied site and finally, the partially occupied sites followed. There was minimal intensity difference between single and multiple occupations at all reflections. Small variations of reflection intensity seemed to have no effect on the proportions of phase relative intensities. The value of lattice parameter for substitution was taken from Ref.14.

Based on the simulation results, it can be concluded that any specific position of the incorporated nickel atoms in the lattice structure does not influence the diffractogram as related to any other positions. However, an increase in the quantity of nickel leads to significant changes in the diffractogram. The more nickel dissolves in the Cu_6Sn_5 intermetallic, the smaller the values of lattice parameters a and c . are. Fig. 4. shows three different simulated diffractation plots. The black curve represents the calculated diffractogram of the nickel-free Cu_6Sn_5 phase, while the blue and the red curves stand for the $\text{Cu}_5\text{Ni}_1\text{Sn}_5$ phase and the $\text{Cu}_4\text{Ni}_2\text{Sn}_5$ phase, respectively. All the reflections shift towards higher angles, which indicates a decrease in lattice parameter a . Another effect of nickel dissolution is the appearance mode of (110) and (102) reflection at $2\Theta = 43^\circ$, and (300) and (212) reflections at $2\Theta = 79$. The two

separate reflections shift to the same position with increase in the nickel content. Due to the decrease of parameter a , reflection (110) shifts towards small values of d . Reflection (300) also shifts towards small values of d , while reflection (212) slightly changes. It can be seen from Nogita's [14] paper that the value of lattice parameter a varies to a larger extent than the value of parameter c .

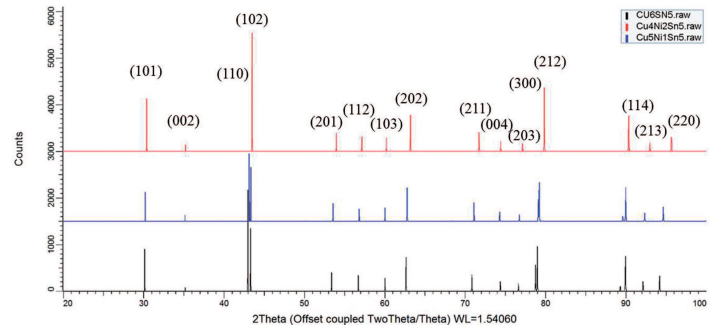


Fig. 4. Simulated diffractograms of the compound phase with different nickel content

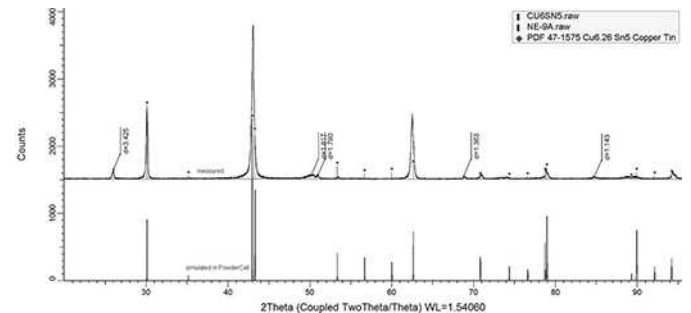


Fig. 5. The evolution of measured pattern and comparison with calculated curves

The diffractograms obtained by simulation can be used as reference models for the identification of intermetallic phases in the qualitative analysis of nickel containing samples.

3.3. Phase analysis of samples with different nickel content

For the Rietveld refinement of nickel alloyed Sn-0.7Cu solders, structural models simulated by PowderCell 2.4 software were used. During fitting, a calculated curve was laid on the measured one, and the degree of fitting of the two curves was tested. After parametric adjustment (cell parameters, crystallite size, preferred orientation, thermal parameters and degree of occupation of atomic positions) the calculated curve was fitted to the measured one. For the identification of the phases present in the sample, the following cards were used from PDF2 database: β -Sn – PDF 004-0673, η - Cu_6Sn_5 – PDF 047-1575. The Rietveld-refinement results of nickel-free Sn-0.7Cu alloy and Sn-0.7Cu alloy with 0.2% nickel content are shown in Figs. 6 and 7, respectively.

The numerical results obtained in Rietveld refinement are found in Table 2.

Results of Rietveld refinement of the Sn-0.7Cu alloys

Alloy	Lattice Parameter, Å		Mean crystallite sizes, nm			Weight fraction, %	
	<i>a</i>	<i>c</i>	Lorentzian FWHM	Integrated Breadth, volume weighted	FWHM, volume weighted	β -Sn	η -Cu ₆ Sn ₅
Sn-0.7Cu	4.2003401	5.0904	173.9	110.739	154.815	98.54	1.46
Sn-0.7Cu-0.025Ni	4.1947923	5.0891012	106.7	67.928	94.963	98.42	1.58
Sn-0.7Cu-0.05Ni	4.1888341	5.0853374	94.5	60.135	84.07	98.34	1.66
Sn-0.7Cu-0.1Ni	4.1816304	5.0729533	52.5	33.418	46.719	96.99	3.01
Sn-0.7Cu-0.2Ni	4.1699863	5.0412682	47.6	30.284	42.337	98.53	1.47

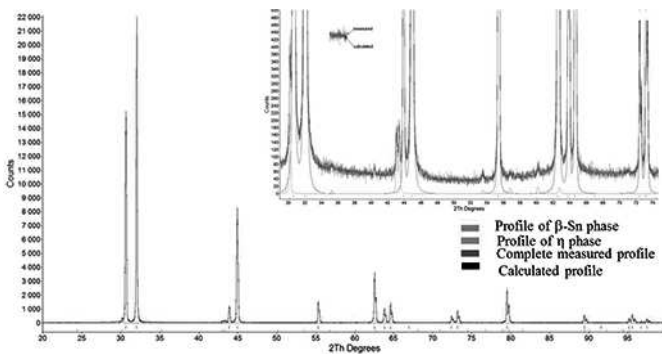


Fig. 6. Rietveld-refinement results of nickel-free Sn-0.7Cu sample

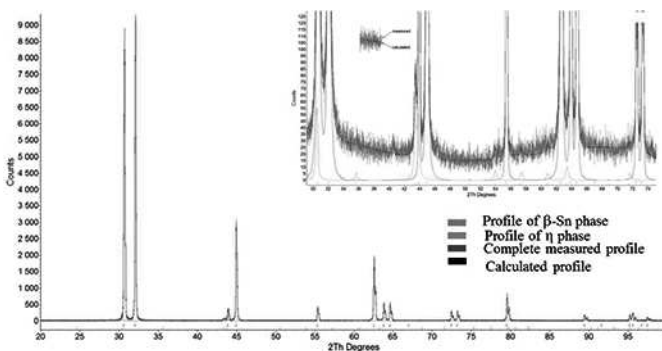
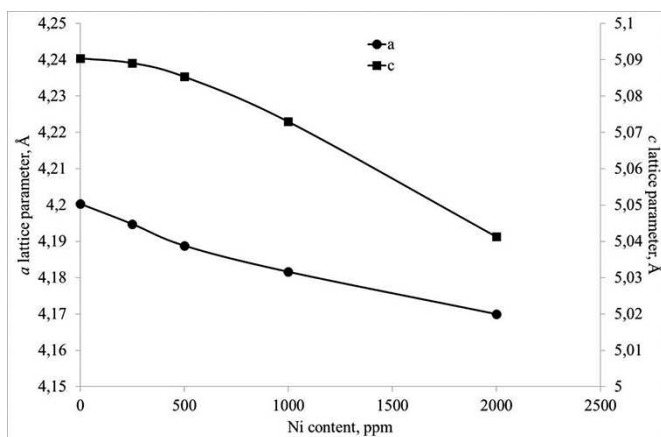


Fig. 7. Rietveld-refinement results of Sn-0.7Cu sample containing 0.2% of nickel

Fig. 8. The lattice parameters of Cu₆Sn₅ in function of the nickel content

By increasing the degree of nickel substitution, the mean crystallite size decreases. Elevated nickel levels leads to a decrease in both *a* and *c* lattice parameters. The variation of lattice parameters as a function of nickel content is shown in Fig. 8.

4. Conclusions

The position of nickel atoms incorporated in the Cu₆Sn₅ phase was simulated by PowderCell 2.4 software. The simulation results can be summarized as follows: (i) the number of atomic positions of nickel incorporation has no discriminant effect on intensity in the diffractograms; (ii) an increase in the nickel content leads to the decrease of lattice parameters *a* and *c* of the Cu₆Sn₅ intermetallic; (iii) the incorporation of nickel in the lattice structure of Sn-0.7Cu leads to a reflection shift towards large angles and to a slight change in reflection intensity.

The behavior of the Cu₆Sn₅ intermetallics in the Sn-0.7Cu lead-free solder is in good agreement with the simulation results. The experimental results show that increased nickel contents lead to a decrease in the mean crystallite size. The novelty of this observation contributes to the literature published so far on the crystalline morphology and structural behavior of intermetallic compounds related to lead-free soldering.

Acknowledgements

This research work of Erzsebet Nagy was supported by the **European Union** and the **State of Hungary, co-financed by the European Social Fund** in the framework of TÁMOP 4.2.4. A/2-11-1-2012-0001 'National Excellence Program'.

The research work of Gyenes Anett, Zoltan Gacsi was based on the results achieved within the TÁMOP-4.2.1.B-10/2/KONV-2010-0001 project and carried out as part of the TÁMOP-4.2.2.A-11/1/KONV-2012-0019 project in the framework of the New Széchenyi Plan. The realization of this project is supported by the European Union, and co-financed by the European Social Fund.

REFERENCES

- [1] ASM Handbook, Volume 3: Alloy phase diagrams, ASM International 1992.

- [2] U.R Kattner, J. Minerals, Metals & Materials Society, **54**, 45 (2002).
- [3] I.T.L. Moura, C.L.M. Silva, N. Cheung, P. R. Goulart, A. Garcia, J.E. Spinelli, Mater Chem Phys. **132**, 203 (2012).
- [4] M. Felberbaum, T. Ventura, M. Rappaz, A.K. Dahle, JOM, 52 (2011).
- [5] T. Ventura, S. Terzi, M. Rappaz, A.K. Dahle, Acta Mater. **59**, 1651 (2011).
- [6] K. Nogita, Intermetallics **18**, 145 (2010).
- [7] A. Gangulee, G.C.Das, M.B.Bever, Metal. Trans. **4**, 2063 (1973).
- [8] A.K. Larsson, L. Stenberg, S. Lidin, Acta Cryst. **B50**, 636 (1994).
- [9] Y.Q. Wu, J.C. Barry, T. Yamamoto, Q.F.Gu, S.D. McDonald, S.Matsumura, H.Huang, K. Nogita, Acta Mater. **60**, 6581 (2012).
- [10] C.M. Gourlay, K. Nogita, J. Read, A.K. Dahle, J Electron Mater. **39**, 1, 56 (2010).
- [11] L. Snugovsky, P Snugovsky, D.D. Perovic, J.W Rutter, Mat. Sci. Tech. **22**, 8, 899 (2006).
- [12] V. Vuorinen, H. Yu, T. Laurila, J.K. Kivilahti, J Electron Mater. **37**, 6, 792 (2008).
- [13] K. Nogita, T. Nishimura, Scripta Mat. **59**, 191 (2008).
- [14] K. Nogita, D. Mu, S.D. McDonald, J. Read, Y.Q. Wu, Intermetallics **26**, 78 (2012).
- [15] C. Yu, J. Liu, H. Lu, P. Li, J. Chen, Intermetallics **15**, 1471 (2007).
- [16] F. Gao, J. Qu, T. Takemoto, J Electron Mater. **39**, 4, 426 (2010).
- [17] A. Paul, C. Ghosh, W.J. Boettinger, Metal. Mater. Trans. **42A**, 952 (2011).